Adsorption of bisphenol A by activated carbon developed from PET by KOH activation

M. Adame-Pereira, M. Alexandre-Franco, C. Fernández-González, V. Gómez-Serrano

[1]Department of Organic and Inorganic Chemistry, University of Extremadura, Badajoz, 06006, Spain

ABSTRACT

This study deals with the preparation of activated carbon (AC) from wasted poly(ethylene terephthalate) (PET) and with the physicochemical characterization of AC and its use as adsorbent of bisphenol A (BPA) in aqueous solution. The preparation of AC was undertaken by the methods of physical activation in steam and chemical activation with KOH. In the chemical activation, the impregnation of PET was carried out by wet and dry routes at the PET:KOH weight ratios of 1:1, 1:3 and 1:5. The ACs were characterized by N_2 adsorption at -196 ºC, mercury porosity, mercury density measurements, FT-IR spectroscopy and measurement of pH of the point of zero charge (pH_{pzc}). Activation yield is 6% with steam and between 23.9 and 75.8% with KOH. Larger surface area and porosity developments are obtained with solid KOH at the impregnation ratio of 1:5 (KS1:5). BET surface area and micropore volume are 1990 $m^2\ g^{-1}$ and 0.41 $cm^3\ g^{-1}$. The pore size distribution in the regions of micro-, meso- and macropores is wider in KS1:5 than in other AC samples. Surface hydroxyl and quinone type structures groups have been analysed in ACs, pH_{pzc} being slightly acidic in character. Adsorption data fit better to the Ho and Mackay second order kinetic model than to the Lagergren first order model and to the Langmuir equation than to the Freundlich equation. From the kinetic and thermodynamic standpoint, the process of BPA adsorption is more favourable for KS1:5.

Keywords: PET, KOH activation, activated carbon, characterization, bisphenol A adsorption.

* Corresponding author: Fax: +34 924 271 149.

E-mail address: vgomez@unex.es (V. Gómez-Serrano).

1. Introduction

At present, the release of a great variety of organic pollutants of industrial origin to environment is a problem of prime importance because of detrimental and pathological effects. One abundant environmental pollutant is bisphenol A (4,4′-(propane-2,2-diyl)diphenol, BPA), which is an organic compound with two hydroxyphenyl groups and that has the chemical formula $C_{15}H_{16}O_2$. BPA is mainly used by the manufacturers as an intermediate in the production of polycarbonate plastics and epoxy resins, flame retardants, and other specialty products [1]. The production of BPA reaches approximately three million tons per year, which is among the highest amounts for chemical products. BPA enters the environment from a variety of sources, mainly including the discharges of industrial wastewater treatment plants, leachates of waste plastic in landfills, processing of BPA in manufacture, and spray paints [1-3]. As a result, it has been detected in all types of environmental water at concentrations ranging from 17.2 mg L^{-1} in hazardous waste landfill leachate [4] to 12 μg L^{-1} in stream water [5] and 3.5–59.8 ng L^{-1} in drinking water [6].

Most environmental organic pollutants are recognized as Endocrine Disruptors Chemicals (EDCs) because of its ability to interfere with the endocrine system. Among the EDCs, BPA was regarded as a representative compound that was first developed as a synthetic estrogen in the 1890s and was reported to have the efficacy of estrogen in stimulating the female

reproductive system in rats in the 1930s. BPA may migrate from interior can coating and polycarbonate containers into food or liquids due to acidic conditions or thermal heat treatment in processing. Food and beverage have been identified as the major sources of human exposure to BPA. In heavily populated areas or industrial sites the contamination by EDCs affects the surface and profound water systems, the surrounding land and drinking waters. Due to its potential health risk, in 1986 the European Union through the Scientific Committee on Food (SCF) allocated a Tolerable Daily Intake (TDI) for BPA at the level 50 μg/kg bw/day. In 2011, the Commission Directive 2011/8/EU prohibited the manufacture of polycarbonated infant feeding bottles with BPA and the import into the EU of such feeding bottles. In 2015, the TDI was lowered down to 4 μg/kg bw/day [7]. In the United State, the Food and Drug Administration (FDA) banned the use of PBA in baby bottles and cups in 2012.

Because of its widespread use and growing evidence that may adversely affect human health [8], the fate of the environmental BPA is an issue of increasing social concern. Accordingly, there is current interest in setting up methods to achieve a fast and effective removal of BPA from various exposure sources. To clean chemically polluted water, conventional methods include reverse osmosis, chemical precipitation, electrochemical treatment, evaporative recovery, ion exchange and adsorption [9]. Of them, adsorption was recognized by the Environmental Protection Agency (EPA) as one of the best methods available to remove organic and inorganic compounds from water intended for human consumption. As the adsorbent, among the various available materials used more frequently with time, activated carbon (AC) has been one of the most important materials from an industrial point of view, having been applied in separation and purification processes of gases and liquids [10]. In fact, AC is a unique and nearly universal adsorbent for such purposes due to its textural properties and surface chemistry, as it possesses a large surface area and well-

developed internal micropore structure as well as a wide spectrum of surface functional groups [11].

Poly(ethylene terephthalate), commonly abbreviated PET, consists of polymerized units of the ($C_{10}H_8O_4$) monomer ethylene terephthalate. PET is a thermoplastic polymer possessing a large number of applications, while most of the world´s production is for synthetic fibers and plastic bottles. Consequently, it is one of the most common synthetic polymers used in our daily life. In recent decades, the PET consumption has undergone a faster-growing rate in the global plastic market due to the expansion of the PET bottle market [12]. As a result, PET has become one of the most abundant municipal and industrial wastes. A few years ago, PET residues on an average were 7.6 wt% of the different polymer wastes generated in Europe [13]. The disposal of large quantities of this waste together with its low bio- and photo-degradability represents a serious challenge for industrial countries worldwide. Disposal options include recovery and recycling, landfilling, co-incineration, and thermal processes [13]. One interesting way of solving the problem of PET disposal is based on its conversion into valuable chemical products such as AC [14-23], i.e., a porous carbon material used mainly as adsorbent of gases, vapours and water-dissolved chemical substances and also as catalyst and catalyst support. The properties of AC depend on the starting material and the method used in its preparation. Desirable starting materials should contain high carbon content and low inorganic matter content, as gathered in the case of PET. This waste material is further abundantly available in a relatively pure state, which would allow PET-based AC to be produced from a variety of feedstock sources, including engineering and municipal wastes. The preparation of AC is usually carried out by the well-known methods of physical activation and chemical activation, which consist of two successive stages of carbonization in N_2 and activation air, carbon dioxide or steam and of impregnation with $ZnCl_2$, H_3PO_4 or KOH and carbonization in N_2, respectively. With PET as the starting material, the chemical

activation with KOH as a way to producing AC has been investigated frequently before [24-28]. In the light of the foregoing, the main objective of this work was to optimize the process of preparation of AC from PET by KOH activation with a view to using such an AC as the adsorbent to remove BPA from water. Preparation is carried out using KOH both in aqueous solution, by allowing for that PET suffers alkaline hydrolysis [29-35], and in solid state in the impregnation of PET impregnation and also by the method of physical activation in steam, for comparison purposes.

2. Materials and methods

2.1. Raw material

Post-consumer 5 L postconsumer mineral water bottles with the trademark "Los Riscos" were used as the PET source. The plastic bottles were first greatly size-reduced by cutting them with laboratory scissors to ≈ 0.5 cm side squared pieces, which were chosen for subsequent studies. After that, PET samples were analysed in a LECO CHNS-932 equipment or incinerated at 650 ºC for 12 h in a muffle furnace. The composition data thus determined are: C, 62.9%; H, 4.3%; N, 0.0%; S, 0.0%, and ash content, 0.0%. As obtained by difference, the oxygen content is equal to 32.9%. The calculated contents of C, H and O from the chemical formula of BPA are 79, 7 and 14%, respectively. All reagents were analytical grade, being used without further purification. Potassium hydroxide (85%, Panreac, Barcelona, Spain) and BPA (Merck) were used.

2.2. Preparation of AC

In previous studies on the preparation of AC by KOH activation, impregnation was carried out using given amounts of PET and KOH in aqueous solution at the PET:KOH weight ratios 1:1 [26], 1:4 [24] and 1:6 [25] or solid KOH at the PET:KOH weight ratios 4:1 [27] and 1:2

[28]. Here, specifically, KOH was used both in aqueous solution and as the commercially furnished solid product, the impregnation PET:KOH weight ratios being 1:1, 1:3 and 1:5. In the first case (i.e., PET impregnation by wet route), 250 mL of KOH solution was brought into contact with 20 g of PET and the liquid/solid phases under steady mechanical agitation were maintained at 85 °C for 2 h. With such a purpose, a three-neck, 500 mL round-bottom glass reactor equipped with a reflux condenser, a mechanical agitator and an electrical heating mantle was used. Once such a time had elapsed, the supernatant liquid was separated by vacuum filtration and the remaining solid was oven-dried at 120 °C for 24 h. In the second case (i.e., PET impregnation by dry route), 2 g of PET and the corresponding amounts of KOH were physically mixed for homogenization, as far as possible. The resulting two series of KOH-impregnated products are noted as KL and KS. Thereafter, above 5 g of each impregnated product was placed in a boat like small size ceramic container and heat-treated in a horizontal cylindrical furnace first dynamically at 10 °C min^{-1} from room temperature to 850 °C and then isothermally at 850 ºC for 2 h in N_2 atmosphere (flow rate = 100 mL min^{-1}). After that, the system was allowed to cool down to room temperature under the same N_2 flow. The resulting products, after extracting the container from the reactor, were thoroughly washed with HCl solution and distilled water to remove the non-reacted KOH and oven-dried at 120 °C for 24 h. By using also 5 g of PET and by heating and cooling under the same conditions, as described before, a single sample of AC was prepared by PET activation in steam atmosphere for comparison purposes. It was performed using a device made up of two in-series closely interconnected horizontal furnaces for the water vaporization and activation treatment (Iberlabo, Madrid, Spain) and of peristaltic pump that continuously propelled a water flow of 40 mL min^{-1} towards the vaporization furnace. The activation methods used in the preparation of AC are summarized in Table 1, together with yield values and sample notations. After preparation, the samples of AC were weighed and stored in airtight plastic containers. The

yield values for the impregnation and activation processes were calculated by the expression (1),

$$Yield\ (I_Y, A_Y) = \frac{M_{AC}}{M_{SM}}\ x\ 100 \qquad (1)$$

where M_{SM} is the starting mass of PET or PET-impregnated/treated product and M_{AC} is the mass of AC and listed in Table 1.

2.3. Characterization of AC

2.3.1. Textural

The textural characterization of samples was accomplished by N_2 adsorption at -196 °C, mercury porosimetry, and mercury density measurements. The N_2 isotherms were determined in a semi-automatic Quantachrome Autosorb-1 equipment. After oven-drying at 120 °C overnight, about 0.15 g of sample was weighed, placed in a glass holder, and out-gassed in the adsorption equipment at 250 °C for 12 h, under a pressure lower than 10^{-3} Torr, prior to effecting the adsorption measurements. From the measured isotherms, the specific surface area (S_{BET}) of the samples was estimated by the Brunauer, Emmet, and Teller equation [36]. The micropore volume (W_0) was calculated by applying the Dubinin-Radushkevich equation [37]. The micropore and mesopore volumes (V_{mi} and V_{me}, respectively) were also obtained by simply reading the adsorbed volumes at p/p° equal to 0.1 and 0.95. All N_2 adsorbed amounts were expressed as liquid volumes for their conversion into pore volumes.

In relation to a complete analysis of the porous structure of solids, as stated by Gregg and Sing [38], the mercury porosimetry method needs to be used in conjunction with the gas adsorption method as the upper limit of this method is in the region of 100-200 Å pore radii. In the present study, a mercury porosimeter (Quantachrome, PoreMaster 60) operating

between 20 and 60000 psi was used in the experiments of mercury intrusion, using ≈ 0.15-0.20 g of sample. This made it possible to determine the cumulative volumes of meso- and macropores (V_{me-p} and V_{ma-p}). The mercury density was measured by mercury displacement of the matter free space present in a volumetric glass holder containing a previously weighted mass of sample. The volume of mercury present in the glass holder to the calibration mark signal was obtained by knowing its mass at the working temperature. Once the mass of sample and its volume was known, the mercury density of sample (ρ_{Hg}) was calculated. The total pore volume (V'_T) was obtained as the summation of W_0, V_{me-p} and V_{ma-p}.

2.3.2. Surface chemistry

The analysis of the surface chemistry of selected samples was carried out by FT-IR spectroscopy and measurement of pH of the point of zero charge (pH_{pzc}) [39]. The FT-IR spectra were recorded on a Perkin-Elmer, Spectrum 100 spectrometer within the range of wavenumbers comprised between 4000 and 400 cm^{-1}, with 50 scans being taken at 2 cm^{-1} resolution. Pellets were prepared by thoroughly mixing a sample of AC and KBr at the 1:1900 carbon/KBr weight ratio in a small size agate mortar, the total mass of the mixture being 238 mg. The resulting mixture was compacted in a Perkin-Elmer manual hydraulic press under a pressure of 10 tons for 3 min. The spectrum of a KBr pellet with the same amount of dispersant as for the PET-AC/KBr pellet was used as the background. pH_{pzc} was measured using 0.01 M NaCl aqueous solutions at pH 2, 4, 6, 8, 10 or 12. These pH values were fixed by adding to the aforesaid solution the requested amount of 0.1 M NaOH or 0.1 M HCl in aqueous solution. In all cases, 5 mL of such solutions were kept in contact with 0.1 g of sample and the system was maintained under continuous stirring for 48 h. Next, the supernatant liquid was separated by filtration prior to measuring its pH. From the plot of pH of the initial solution (pH_i) against pH of the supernatant (pH_f), pH_{pzc} was obtained as the intersection of such a plot with the $pH_i = pH_f$ plot, as shown in Fig. 1.

2.5. Adsorption of BPA

In the study of the adsorption process of BPA in aqueous solution only VA and the KS samples were used as adsorbents since, as shown by preliminary results, adsorption was practically negligible with the KL samples. Adsorption experiments were carried out by the batch procedure. A Selecta Thermostatic shaker bath (Unitronic-ORC) filled with water at 25 °C and shaken at 50 oscillations per minute was used throughout the experiments. BPA is a moderately water-soluble compound (i.e., 300 mg L^{-1}/1.31 mol L^{-1} at room temperature) [40], which determined the concentration of the BPA solution and the amount of adsorbent used in the adsorption tests. Accordingly, a 10^{-3} mol L^{-1} BPA stock solution was prepared. pH of this solution was 6.22, as measured in a Crison pH-Meter 21. The reported pK_a1 and pK_a2 for the BPA dissociation to an anionic or di-anionic species are 9.6 and 10.2 [1, 41]. In a typical adsorption kinetic experiment, a fixed amount (≈ 0.01 g) of adsorbent and 25 mL of BPA solution were added to a set of 25 mL glass test tubes, provided with Bakelite screw-up caps. The contact between the liquid and solid phases was maintained for different time intervals, ranging between 1 min and several, BPA in the supernatant liquid was determined. For the definition of the adsorption equilibrium isotherms, 25 mL of aqueous solution of BPA solution were kept in contact a varying amount of adsorbent ranging between 0.008 and 0.02 g for a period of time longer than that strictly necessary to equilibration was reached in the adsorption system. The concentration of BPA was analysed by UV-Vis spectrophotometry in an UV-1800 Shimadzu equipment. It was found that BPA is stable in aqueous solution for the time period of a typical experiment. After registering the absorption spectrum in the UV-Vis region and verifying that the absorbance against concentration data obeyed well the Beer´s law, absorbance measurements were performed thereafter at 276 nm.

3. Results and discussion

3.1. Preparation of AC. Process yield

3.1.1. Wet impregnation stage

The yield values for the impregnation process of PET listed in Table 1 indicate that the mass of PET noticeably decreased after its contact with the KOH solutions. Also, notice that the mass decrease was significantly higher with increasing impregnation ratio. Probably, the main factor influencing the mass of sample was the alkaline hydrolysis of PET, i.e., ester bonds in the PET are cleaved by the nucleophilic attack of hydroxide ions under the formation of the di-potassium terephthalate salt and ethylene glycol, which are both soluble in the aqueous phase [42], i.e., ethylene glycol is miscible with water. In connection with the alkaline hydrolysis of PET it has been stated previously that almost complete conversion of PET occurs in relatively mild process conditions. Thus, it leads to the total depolymerisation of PET to its monomers in reaction times ranging from a few to 30 min at high temperature and under high pressures, and requires no additives, such as catalysts or neutralizers [34, and refers therein]. Nevertheless, heat treatment temperatures between 120 and 200 ºC and reaction times of 1-7 h have been reported before [32]. Therefore, the high yields in the range ≈ 96-76% obtained in this study can be accounted for by the less severe heating conditions of 85 ºC for 2 h at atmospheric pressure used when PET was chemically treated with the KOH aqueous solutions. The increase produced in the mass loss of PET with increasing PET:KOH ratio is consistent with the stoichiometry of the hydrolysis reaction, which takes place between two mol of KOH and one mol of BPA and that therefore was more favourable with a greater presence of KOH in the reaction medium. Therefore, only when the 1:3 and 1:5 PET:KOH ratios were used, KOH was really in excess with respect to PET. After soaking at 85 ºC for 2 h, the unreacted KOH to a large extent should be removed by filtration of the residual aqueous liquid. Finally it should be mentioned that, based on the basic hydrolysis of PET, a method of preparation of activated carbons has been developed before consisting of

the stages of PET complete de-polymerization, filtration, water evaporation, and solid carbonization [25].

3.1.2. Activation stage

In the case of the activation stage, mass balance data given in Table 1 show that yield is strongly dependent on the method used in the overall process of preparation of AC from PET. First, yield is much higher when it was carried by chemical activation with KOH than by physical activation in steam. Second, it is noticeably dependent on whether the impregnation was effected by the wet or dry route according to the PET:KOH ratio; being higher and lower at a low and at higher impregnation ratios, respectively. Third, yield greatly decreases in increasing impregnation ratio, being as low as 23.9% at most for KS1:5. Nevertheless, this yield is however significantly higher than 17.1% obtained for the pyrolysis of PET at 900 ºC for 2 h in N_2, which was performed in an aside experiment. Furthermore, it is worth noting that the yield of 38.1% for KS1:3 compares with those obtained for the preparation of AC from a lignocellulosic material as cherry stone by chemical activation with H_3PO_4 [43]. Since AC is frequently prepared from woody materials it is also relevant to point out here that the yield of the carbonization, which followed by the activation, of cherry stone was 26.3 and 25.4 % when heating from ambient temperature to 600 ºC in the atmosphere of the pyrolysis products and in N_2, respectively [44]. Therefore, the relatively high yield for the preparation of AC from PET is an interesting finding as the economic analyses of AC plants are very sensitive to activation route and production yield [22].

3.2. Textural characterization

3.2.1. Surface area, micro- and mesoporosity

The adsorption isotherms of N_2 at -196 ºC measured for the several samples of AC, which were prepared as described above, are shown in Fig. 2. In accordance with the BDDT classification system based on the shape of the N_2 isotherms, such isotherms resemble composite Type I and IV isotherms for VA and the KS samples and Type II and IV isotherms for the KL samples. Accordingly, adsorption must occur in micro- and mesopores for the former samples and on external surface and large size pores for the latter samples. Furthermore, the wider pore-size distribution in the regions of micro- and mesopores for KS1:5 than for the rest of ACs is worth noting. As shown by the values of S_{BET} and pore volumes obtained from the N_2 isotherms (see Table 2), S_{BET} and W_0 are much higher for KS1:5 than for VA but similar for KS1:1 and VA. Furthermore, S_{BET} and W_0 are as high as 1990 $m^2\ g^{-1}$ and 0.71 $cm^3\ g^{-1}$ for KS1:5 and by contrast they are as low as 12 $m^2\ g^{-1}$ and 0.0 $cm^3\ g^{-1}$ for KL1:5. For ACs prepared by wet impregnation of PET with KOH, S_{BET} was between 472 and 1391 $m^2\ g^{-1}$ [24-26], which are by far lower than 1990 $m^2\ g^{-1}$ for KS1:5 and that prove the use of solid KOH in the preparation of AC had a marked beneficial effect on the creation of microporosity. Moreover, S_{BET} and W_0 greatly increase with the increase in the content of KOH in the impregnation mixture, which is also worthy to be highlighted. In summary, from the results obtained in the textural characterization of AC by N_2 adsorption at -196 ºC it follows therefore that the degree of development of the surface area and microporosity is larger by activating with KOH than in steam, impregnating with solid KOH instead of with KOH in aqueous solution, and increasing the content of KOH in this solution. In brief, the textural effects associated with the activation process of PET or KOH-impregnated PET are more favourable by the order KS > VA >> KL and KS1:5 > KS1:3 > KS1:1.

3.2.2. Meso- and macroporosity

The curves of mercury intrusion, which are graphically plotted in Fig. 3, reveal that the pore size distribution in the region of macro- or mesopores is wider for the KS samples and for KS1:5 and VA, respectively. The presence of varying size macropores in the KL samples is also worthwhile noting. As can be seen in Table 3, $V_{me\text{-}p}$ is 0.81 $cm^3\ g^{-1}$ for KS1:5 and $V_{ma\text{-}p}$ is 2.11 $cm^3\ g^{-1}$ for KS1:3. For the KL samples, however, $V_{me\text{-}p}$ and $V_{me\text{-}p}$ are 0.13 and 0.38 $cm^3\ g^{-1}$ in the case of KL1:1 at most. Nevertheless, it should be mentioned that the KL samples are much more macroporous than mesoporous ACs. The opposite is however true for VA, as $V_{me\text{-}p}$ is 0.36 $cm^3\ g^{-1}$ and $V_{ma\text{-}p}$ is 0.08 $cm^3\ g^{-1}$ for this sample. In short, from the above results it becomes apparent that by using PET as feedstock the preparation of AC with a more or less heterogeneous porosity by KS samples > VA > KL samples is feasible, which is an interesting finding with a view to preparing AC with a tailored porous structure.

3.2.3. Total porosity

The mercury density (ρ_{Hg}), or apparent density, of a solid is the weight of one millilitre of solid granules, excluding the volume of the interstitial space between them [45]. Therefore, the value of ρ_{Hg} (g cm^{-3}), or better of ρ_{Hg}^{-1} ($cm^3\ g^{-1}$), may be regarded as a rough estimate of the total porosity present in a porous solid, embracing even narrower pores that are not accessible to small gas molecules, such as He and N_2. Although mercury does not wet porous solids such as AC, the use of ρ_{Hg} for such as purpose is somehow handicapped by the presence of large size pores which are filled with mercury prior applying pressure in the porosimeter. The reported ρ_{Hg} densities are usually from 0.6 to 0.8 g cm^{-3} [45]. Data in Table 3 show in fact that ρ_{Hg} is notably higher for the KL samples than for the KS samples, which is in line with the unequal porosity development in both series of samples. This is also evident from the V'_T values (see Table 3), which range between 0.43 and 0.57 $cm^3\ g^{-1}$ for the former samples and between 2.21 and 3.29 $cm^3\ g^{-1}$ for the latter samples. The so high ρ_{Hg} measured for VA appears to be striking as V'_T is 0.91 $cm^3\ g^{-1}$ for this sample, which is markedly higher

than for the KL samples and lower than for the KS samples. However, it is worth noting that the values of ρ_{Hg}^{-1} and V'_T are fairly close for VA and the KS samples, in particular for KS1:3 with ρ_{Hg}^{-1} and V'_T equal to 3.23 $cm^3\ g^{-1}$ and 3.25 $cm^3\ g^{-1}$, respectively. The much higher ρ_{Hg}^{-1} than V'_T for the KL samples argues for an important presence of small pores in the KL samples, which are not accessible to N_2(g) at -196 ºC.

3.3. Surface chemistry study

3.3.1. By FT-IR spectroscopy

The FT-IR spectra registered between 4000 and 400 cm^{-1} for VA, KS1:3 and KS1:5 AC (Fig. 4) show a series of stronger absorption bands of varying intensity with their absorption maximum located in the neighbourhoods of 3700, 1675, 1460 (i.e., this band is broad and has a shoulder at higher frequencies) or 1014 cm^{-1}, which are ascribable in turn to the ν(O-H) vibration of hydroxyl groups, ν(C=O) vibration of quinone type structures rather than to the same bond vibration mode in carboxylic acid groups, ν(C=C) skeletal of aromatic rings and $\delta_a(CH_2)$ of $–CH_2-$ groups, ν(C-O) vibration of hydroxyl groups/ether type structures. Notice that only the spectrum of VA displays the broad band around 3431 cm^{-1}. This band may also be assigned to the ν(O-H) vibration hydroxyl groups which, unlike the -OH absorbing at higher frequencies, are probably involved in hydrogen bonding. On the other hand, the weak bands at 2932 and 2860 cm^{-1} are readily visible only in the spectra of VA and KS1:3, being attributable to the ν_a(C-H) vibration and ν_s(C-H) vibration of $-CH_2-$ groups. Band intensities indicate that a greater presence of H-bonded –OH groups and $–CH_2–$ groups in VA and of C=O groups and C=C bonds containing rings in KS1:3 and especially in KS1:5. Symbols mean: ν, stretching, δ, bending; a, asymmetrical; s, symmetrical.

3.3.2. By pH_{pzc} measurement

The pH_{pzc} values obtained for all AC samples are given in Table 4. As can be seen, pH_{pzc} is either slightly higher or lower than 7.00, which is consistent with the presence of weak acidic –OH surface groups in the samples analysed by FT-IR. Furthermore, pH_{pzc} varies by VA (7.20) > KL samples (≈ 6.35-6.25) > KS samples (≈ 5.70-5.35). The sequence of pH_{pzc} variation must be kept in mind in connection with the results of BPA adsorption since the pH_{pzc} value indicates the pH at which the surface of an AC changes its charge from positive to negative, which influences the adsorption of charged adsorptives from aqueous solution.

3.4. Adsorption of BPA

3.4.1. Kinetics

The concentration (C x 10^3, mol L^{-1}) vs. time (t, h) plots obtained for the selected adsorption systems are depicted in Fig. 5. From this figure it follows first that, in general, the adsorption kinetics of BPA is fast, as the time needed to equilibration in such systems is shorter than approximately 50 h. Nevertheless, it depends on each adsorbent, as inferred from the slope of the descending branch in such plots. Thus, the C decrease at short adsorption times is greater for VA, KS1:3 and KS1:5 than for KS1:1. However, after a contact time between the solid and liquid phases of only a few hours the initial concentration of the BPA solution (C_0 x 10^3, mol L^{-1}) is reduced to ≈ 30% with KS1:3 and KS1:5 and to ≈ 70% with VA and KS1:1. Therefore, from these results it can be tentatively stated that adsorption process was speeded up for KS1:3 and KS1:5 as compared to KS1:1 and VA. The behaviour exhibited by the various adsorbent samples, regarding the kinetics of the adsorption process, is in line with their mesoporous structure, as described above. Thus, the pore size distribution in the region of mesopres is wider for VA and KS1:5, though the mesopore volume is higher for KS1:3 and KS1:5 (see data in Table 3). Also, it should be noted that the degree of development of macroporosity is larger for KS1:3 and KS1:5 than for KS1:1 and especially

for VA. As is well known, meso- and macropores are the pores that control of the internal diffusion of the adsorptive to the micropores, which is where most adsorption active sites concentrate in adsorbents with a large surface area as AC.

The kinetic data have been fitted to the Lagergren equation [46] (pseudo-first order kinetic model) and to the Ho and Mackay equation [47] (pseudo-second order kinetic model). The integrated Lagergren equation in linear form is:

$$log(q_e - q_t) = logq_e - \frac{K_1}{2.303}t \qquad (2)$$

where q_t and q_e are the amounts adsorbed at time t and at equilibrium (mol g^{-1}), respectively, and k_1 is the pseudo-first order rate constant (h^{-1}). The plot of log (q_e–q_t) versus t should therefore be a straight line with slope log q_e and intercept –k_1/2.303.

The pseudo-second order equation is:

$$\frac{t}{q_t} = \frac{1}{K_2 q_e^2} + \frac{1}{q_e}t \qquad (3)$$

where q_e and q_t are the adsorption capacities at equilibrium and time t, respectively (mol g^{-1}) and k_2 is the rate constant of pseudo-second order adsorption (g mol^{-1} h^{-1}). Here, the plot of t/q_t against t should give a linear relationship, from which q_e, k_2 can be obtained from the slope and intercept of the plot.

The estimated values of q_e, k_1, k_2 and R are listed in Table 5. In general, the kinetic data fit better to the pseudo-second order kinetic model than to the pseudo-first order kinetic model, as in the first case the values of R are very close to unity for all adsorption systems. Furthermore, as expected, k_2 is higher by the order KS1:5 > VA > KS1:3 > KS1:1. Therefore, it seems that the textural parameter that controls the kinetics of the adsorption process of BPA

is the pore size distribution of the adsorbent in the region of mesopores, which is wider (see Fig. 3) just in accord with the aforesaid variation sequence of k_2.

3.4.2. Adsorption isotherms

The adsorption isotherms of BPA in dilute aqueous solution on the selected AC samples are plotted in Fig. 6. At a glance they show that, practically in the entire range of C_e/C_0 (i.e., C_e and C_0 are the equilibrium and initial concentrations of BPA), adsorption is higher by KS1:5 > KS1:3 > VA > KS1:1. Furthermore, it is substantial at C_e/C_0 = 0.0 and increases at higher C_e/C_0, but especially above C_e/C_0 > 0.8 for a larger number of samples. A well-defined long isotherm plateau is not observed for most samples, except for KS1:1. Regarding the isotherm shapes, they resemble the H curve of the Giles´s classification system of solution adsorption systems [48]. Therefore, it is indicative of a high affinity of the solute in a dilute solution for the adsorbent in such a way that it is completely adsorbed at low C_e/C_0 and also that adsorption is flat. This adsorption is consistent with the geometry of the BPA molecule, which is 3.83, 5.87 and 10.68 Å [49] and hence it should prefer accommodating flat rather than end-on on the surface of narrow pores as the micropores, which are less than ≈ 20 Å in width [38]. It is further supported by pH_{pzc} of the adsorbent, pH of the BPA solution, and pK_a of BPA dissolved in water. Correspondingly, both the surface groups and structures of the adsorbent and BPA are both slightly acidic in character and therefore they would remain practically undissociated after the contact of the BPA solution with the adsorbent was established. Consequently, the hydrophobic and π-π molecular interactions should prevail over the ion-ion electrostatic interactions, BPA adsorbing then flat. In fact, possible hydrophobic groups/hydrophilic groups, as shown schematically before for ibuprofen [50], and electron-donating-nucleophilic groups/electron-withdrawing-electrophilic groups involved in adsorption interactions are present in both the ACs and the BPA. On the other

hand, a short plateau must mean that the adsorbed solute molecules expose a surface which has nearly the same affinity as the original surface had. Moreover, the second adsorption rise, which starts at a very different C_e/C_0 depending on the sample, argues for multilayer adsorption or on fresh surface [48]. In this connection it is relevant to point out here that, as shown the knee of the N_2 adsorption isotherms (see Fig. 2), is wider by KS1:5 > KS1:3 > KS1:1 > VA and therefore multilayer adsorption would be a more favourable process with increasing pore size.

From the data of adsorption equilibrium for BPA, i.e., $q_e=f(C_e/C_0)$, it is possible to obtain valuable information about the adsorption process. For this purpose, the adsorption isotherm is adjusted to different theoretical models in order to offer the parameters of the process which allow characterization and to establish comparisons deemed appropriate. In the present study, the aforesaid data have been adjusted according to Langmuir and Freundlich equations. The Langmuir model [51] has been widely used to describe the monolayer adsorption occurring on homogenous surface with a finite number of identical adsorption sites, which can be represented by the following equation:

$$q_e = \frac{Q_0 b C_e}{1+bC_e} \qquad (4)$$

where q_e is the amount of BPA uptaken per unit mass of adsorbent (mol g^{-1}), C_e is the equilibrium concentration of the adsorptive solution in contact with adsorbent (mol L^{-1}), Q_0 the adsorption capacity pertaining to the formation of the monolayer (mol g^{-1}) and b a constant related to the adsorption energy ($b \propto e^{-\Delta H/RT}$). Frequently, equation (4) is rearranged in the form:

$$\frac{C_e}{q_e} = \frac{1}{Q_0 b} + \frac{C_e}{Q_0} \qquad (5)$$

the plot of C_e/q_e (g L^{-1}) versus C_e (mol L^{-1}) should give a linear relationship, from which $1/Q_0$ and $1/Q_0b$ can be obtained from the slope and intercept of the plot.

One of the major characteristics of the Langmuir isotherm is that may be expressed in terms of equilibrium parameter (R_L), which is a dimensionless constant referred to as separation factor or equilibrium parameter, defined by Weber and Chakravorti [52] as:

$$R_L = \frac{1}{1+bC_0} \quad (6)$$

where b is the Langmuir constant and C_0 is the initial concentration of the adsorbate solution. R_L value indicate the adsorption nature: un favourable if $R_L>1$, linear if R=1, favourable if $0 < R_L < 1$ and irreversible if $R_L=0$.

The Freundlich isotherm [53] was one of the first equations proposals to associate the adsorbed amount of a chemical species by a given amount of adsorbent with the concentration of that species in the solution. These data often fit the next equation put forward by Freundlich at the beginning of the last century:

$$q_e = K_F C_e^{\frac{1}{n}} \quad (7)$$

where q_e is the amount retained of solute per gram of the adsorbent (mol g^{-1}) at equilibrium, C_e is the equilibrium concentration (mol L^{-1}), K_F and 1/n ($0 < 1/n < 1$) are constants related to the adsorption capacity of the adsorbent and the adsorption intensity. The values of these constants can be obtained from the following expression:

$$logq_e = logK_F + \frac{1}{n} logC_e \quad (8)$$

with 1/n and K_F being computed from the slope and intercept of the Freundlich plot of log q_e against log C_e.

The resulting values of the isotherm parameters of Langmuir and Freundlich (n, K_F, Q_0, b) and fitting coefficient (R) are listed in Table 6. The values of R indicate that adsorption isotherms of BPA as a rule fits more satisfactorily to the Langmuir isotherm model than to the Freundlich isotherm model, except for KS1:1. It was expected in view of the PET chemical composition since it is constituted of carbon, hydrogen and oxygen and by thermal decomposition should become transformed into a product with a very homogeneous surface. Furthermore, R_L is > 0 and < 1 and further low and therefore the adsorption process appears to be favourable and rather irreversible. Moreover, Q_0 varies by KS1:5 >> VA ≈ KS1:3 > KS1:1, as inferred also from the adsorption isotherms plotted in Fig. 6.

4. Conclusions

From the results obtained in the present study focused on the preparation of AC from wasted PET and on the physiochemical characterization of the resulting AC and its use as adsorbent of BPA in aqueous solution, the following conclusions may be drawn. The yield of the process of preparation of AC from PET by KOH activation is high, regardless of whether impregnation is effected by the wet or dry route. Activation yield is 6% with steam and 23.9-75.8% with KOH. Because of the hydrolysis and subsequent filtration of KOH containing residual liquid, the impregnation of PET with KOH in aqueous solution is not effective at all to generate microporosity in the subsequent heat treatment of the residual solid at high temperature but the resulting ACs are essentially macroporous solids. By impregnating PET with solid KOH, AC with a more heterogeneous porosity in the regions of micro-, meso- and macropores is obtained. The pore size distribution is wider when using and increased impregnation ratio. For KS1:5, S_{BET} is 1990 $m^2\ g^{-1}$ and W_0 is 0.71 $cm^3\ g^{-1}$. In addition, $V_{me\text{-}p}$ is 0.81 $cm^3\ g^{-1}$ and $V_{ma\text{-}p}$ is 1.77 $cm^3\ g^{-1}$. For VA, S_{BET} and the pore volumes are markedly smaller. Surface hydroxyl and quinone type groups have been analysed in ACs, pH_{pzc} being only slightly different from 7.00. Adsorption data fit better to the Ho and Mackay second

order kinetic model than to the Lagergren first order model and to the Langmuir equation than to the Freundlich equation. From the kinetic and thermodynamic standpoint, the process of BPA adsorption is more favourable for AC prepared from PET by chemical activation with solid KOH, especially when the PET:KOH ratio of 1:5 was used in the impregnation of PET. The kinetic constant k_2 is 526 g mol^{-1} h^{-1} and the equilibrium parameter Q_0 is 425 x 10^{-3} mol g^{-1} for KS1:5. 2In general, the behaviour of AC in the adsorption of PBA is consistent with adsorbent textural properties, especially the meso- and micropore size distributions.

Acknowledgements

Financial support from the Junta de Extremadura through European Funds for Regional Development (ERDF) by the Aid to Research Groups (GR18013) is gratefully acknowledged.

Reference

[1] Staples, C.A., Dorn, P.B., Klecka, G.M., O´Block, S.T., Harris, L.R.: A review on the environmental fate, effects, and exposures of bisphenol A. Chemosphere 36, 2149-73 (1998).

[2] Yamamoto, T., Yasuhara, A., Shiraishi, H., Nakasugi, O.: Bisphenol A in hazardous waste landfill leachates. Chemosphere 42, 415–418 (2001).

[3] Cousins, I.T., Staples, C.A., Klecka, G.M., Mackay, D.: A multimedia assessment of the environmental fate of bisphenol A. Hum. Ecol. Risk Assess. 8, 1107–1135 (2002).

[4] Bautista-Toledo, M.I., Rivera-Utrilla, J., Ocampo-Pérez, R., Carrasco-Marín, F., Sánchez-Polo, M.: Coop erative adsorption of bisphenol-A and chromium(III) ions from water on activated carbons prepared from olive-mill waste. Carbon 73, 338-350 (2014).

[5] Liu, G., Ma, J., Li, X., Qin, Q.: Adsorption of bisphenol A from aqueous solution onto activated carbons with different modification treatments. J. Hazard. Mater. 164, 1275–1280 (2009).

[6] Santhi, V.A., Sakai, N., Ahmad, E.D., Mustafa, A.M.: Occurrence of bisphenol A in surface water, drinking water and plasma from Malaysia with exposure assessment from consumption of drinking water. Sci. Total Environ. 427–428, 332–338 (2012).

[7] Cwiek-Ludwicka, K.C.: Bisphenol A (BPA) in food contact materials – new scientific opinion from EFSA regarding public health risk. Rocz. Panstw. Zakl. Hi. 66, 299-307 (2015).

[8] Rochester, J.R.: Bisphenol A and human health: A review of the literature. Reprod. Toxicol. 42, 132-155 (2013).

[9] Pellera, F.-M., Giannis, A., Kalderis, D., Anastasiadou, K., Stegmann, R., Wang, J.-Y., Gidarakos, E.: Adsorption of Cu(II) ions from aqueous solutions on biochars prepared from agricultural by–products. J. Environ. Manage. 96, 5–42 (2012).

[10] Molina-Sabio, M., Rodríguez-Reinoso, F., Caturla, F., Sellés, M.J.: Porosity in granular carbons activated with phosphoric acid. Carbon 33, 1105–1113 (1995).

[11] Radovic, L.R., Moreno-Castilla, C., Rivera-Utrilla, J.: Materials as adsorbents in aqueous solutions. In: Radovic, L.R. (ed.) Chemistry and Physics of Carbon, pp. 227–405. Marcel Dekker, New York (2001).

[12] Association of Plastic Manufacturers in Europe. An analysis of plastics consumption and recovery in Western Europe; 2001.

[13] Brems, A., Baeyens, J., Vandecasteele, C., Dewil, R.: Polymeric cracking of waste polyethylene terephthalate to chemicals and energy. J. Air & Waste Manage. Assoc. 61, 721-731 (2001).

[14] Bóta, A., László, K., Nagy, L.G., Copìtzky, T.: Comparative study of active carbons from different precursors. Langmuir 13, 6502-6509 (1997).

[15] László, K., Bóta, A., Nagy, L.G., Cabasso, I.: Porous carbons from polymer waste materials. Colloids Surf., A 151, 311-320 (1999).

[16] Marzec, M., Tryba, B., Kalenczuk, R.J., Morawski, A.W.: Poly(ethylene terephthalate) as a source for activated carbon. Polym. Adv. Technol. 10, 588–595 (1999).

[17] Kartel, N.T., Gerasimenko, N.V., Tsyba, N.N., Nikolaichuk, A.D., Kovtun, G.A.: Synthesis and study of carbon sorbent prepared from polyethylene terephthalate. Russ. J. Appl. Chem. 74, 1765–1767 (2001).

[18] Parra, J.B., Ania, C.O., Arenillas, A., Pis, J.J.: Textural characterization of activated carbons obtained from poly(ethylene terephthalate) by carbon dioxide activation. Stud. Surf. Sci. Catal. 144, 537–543 (2002).

[19] Nakagawa, K., Namba, A., Mukai, S.R., Tamon, H., Ariyadejwanich, P., Tanthapanichakoon, W.: Adsorption of phenol and reactive dye from aqueous solution on activated carbons derived from solid wastes. Water Res. 38, 1791–1798 (2004).

[20] Fernández-Morales, I., Almazán-Almazán, M.C., Pérez-Mendoza, M., Domingo-García, M., López-Garzón,F.J.: PET as precursor of microporous carbons: preparation and characterization. Microporous and Mesoporous Mater. 80, 107–115 (2005).

[21] Dias, J.M., Alvim-Ferraz, M.C.M., Almeida, M.F., Rivera-Utrilla, J., Sanchez-Polo, M.: Waste materials for activated carbon preparation and its use in aqueous phase treatment: a review. J. Environ. Manage. 85, 833–846 (2007).

[22] Bazargan, A., Hui, C.W., Mckay, G.: Porous carbons from plastic waste. Adv. Polym. Sci. (2013). doi: 10.1007/12_2013_253.

[23] Bratek, W., Swiatkowski, A., Pakula, M., Biniak, S., Bystrzejewski, M., Szmigielski, R.: Characteristics of activated carbon prepared from waste PET by carbon dioxide activation. J. Anal. Appl. Pyrol. 100, 192-198 (2013).

[24] Arenillas, A., Rubiera, F., Parra, J.B., Ania, C.O., Pis, J.J.: Surface modification of low cost carbons for their application in the environmental protection. Appl. Surf. Sci. 252, 619-624 (2005).

[25] Almazán-Almazán, M.C., Pérez-Mendoza, M., López-Domingo, F.J., Fernández-Morales, I., Domingo-García, M., López-Garzón, F.J.: A new method to obtain microporous carbons from PET: Characterization by adsorption and molecular simulation. Microporous and Mesoporous Mater. 106, 219-228 (2007).

[26] Adibfar, M., Kaghazchi, T., Asasian, N., Soleimani, M.: Conversion of poly(ethylene terephthalate) waste into activated carbon: chemical activation and characterization. Chem. Eng. Technol. 37, 979-986 (2014).

[27] Djahed, B., Shahsavani, E., Naji, F.K., Mahvi, A.H.: A novel and inexpensive method for producing activated carbon from waste polyethylene terephthalate bottles and using it to remove methylene blue dye from aqueous solution. Desalin. Water Treat. (2015). doi: 10.1080/19443994.2015.1033647.

[28] Mendoza-Carrasco, R., Cuerda-Correa, E.M., Alexandre-Franco, M.F., Fernández–González, C., Gómez-Serrano, V.: J Environ. Manage. 18, 522-35 (2016).

[29] Paszun, D., Spychaj, C: Chemical recycling of poly(ethylene terphthalate). Ind. Eng. Chem. Res. 36, 1373-1383 (1997).

[30] Kaufman, D., Wright, G., Kroemer, R., Engel, J.:“New” compounds from old plastics: recycling PET plastics via depolymerization. J. Chem. Educ. 76, 1525-1526 (1999).

[31] Wan, B.-Z., Kao, C.-Y., Cheng, W.-H.: Kinetics of depolymerization of poly(ethylene terephthalate) in a potassium hydroxide solution. Ind. Eng. Chem. Res. 40, 509-514 (2001).

[32] Karayannidis, G.P., Chatziavgoustis, A.P., Achilias, D.S.: Poly(ethylene terephthalate) recycling and recovery of pure terephthalic acid by alkalyne hydrolysis. Adv. Polym. Technol. 21, 250-259 (2002).

[33] Kumar, S., Guria, C.: Alkaline hydrolysis of waste poly(ethylene terephthalate): a modified shrinking core model. J. Macromol. Sci., Part A. (2005). doi. 10.1081/MA-200050346.

[34] Spaseska, D., Civkaroska, M.: Alkaline hydrolysis of poly(ethylene terephthalate) recycled from the postconsumer soft-drink bottles. J. Univ, Chem. Technol. Metal. 45, 379-384 (2010).

[35] Yamashita, M., Mukai, H.: Alkaline hydrolysis of polyethylene terephthalate at lower reaction temperature. Sci. Eng. Rev. Doshisha Univ. 52, 51-56 (2011).

[36] Brunauer, S., Emmett, P., Teller, E.: Adsorption of gases in multimolecular layers. J. Am. Chem. Soc. 60, 309-319 (1938).

[37] Dubinin, M.M.: Physical adsorption of gases and vapors in micropores. In: Cadenhead, D.A., Danielli, J.F., Rosenberg, M.D. (eds.) Progress in Surface and Membrane Science, pp. 1-70, Academic Press, New York (1975).

[38] Gregg, S.J., Sing, K.S.W.: Adsorption, Surface Area and Porosity. Academic Press, London (1982).

[39] Lopez-Ramon, M., Stoeckli, F., Moreno-Castilla, C., Carrasco-Marin, F.: On the characterization of acidic and basic surface sites on carbons by various techniques. Carbon 37, 1215-1221 (1999).

[40] Rykowska, I., Wasiak, W.: Properties, threats, and methods of analysis of bisphenol A and its derivatives. Acta Chromatogr. 16, 7-27 (2006).

[41] Tay, K.S., Rahman, N.A., Abas, M.R.B.: Degradation of bisphenol A by ozonation: rate constants, influence of inorganic anions, and by-products. Maejo Int. J. Sci. Technol. 6, 79-94 (2012).

[42] Palme, A., Peterson, A., de la Motte, H., Theliander, H., Brelid, H.: Development of an efficient route for combined recycling of PET and cotton from mixed fabrics. Text. Clothing Sustain. (2017). doi: 10.1186/s40689-017-0026-9.

[43] Olivares-Marín, M., Fernández-González, C., Macías-García, A., Gómez-Serrano, V.: Porous structure of activated carbon prepared from cherry stones by chemical activation with phosphoric acid. Energy Fuels 21, 2942-2949 (2007).

[44] Durán-Valle, C.J., Gómez-Corzo, M., Pastor-Villegas, J., Gómez-Serrano, V.: Study of cherry stones as raw material in preparation of carbonaceous adsorbents. J. Anal. Appl. Pyrolysis 73, 59-67 (2005).

[45] Smisek, M., Cerny, S.: Active Carbon: Manufacture, Properties and Applications. Elsevier, Amsterdam (1970).

[46] Lagergren, S.: About the theory so-called adsorption of soluble substances. Kungliga Svenska Vetenskapsakademiens Handllingar 24, 1-39 (1898).

[47] Ho, Y., McKay, G.: Pseudo-second order model for sorption processes. Process Biochem. 34, 451-465 (1999).

[48] Giles, C.H., MacEwan, T.H., Nakhwa, S.N., Smith, D.: Studies in adsorption. Part XI. A system of classification of solution adsorption isotherms, and its use in diagnosis of adsorption mechanisms and in measurement of specific surface areas of solids. J. Chem. Soc, London 111, 3973-3993 (1960).

[49] Schäfer, A.I., Nghiem, L.D., Oschmann, N.: Bisphenol A retention in the direct ultrafiltration of greywater. J. Membr. Sci. (2006). doi: 10.1016/j.memsci.2006.06.035

[50] Dwivedi, A.D., Gopal, K., Jain, R.: Strengthening adsorption characteristics of non-steroidal anti-inflammatory drug onto microwave-assisted mesoporous material: process design, mechanism and characterization. Chem. Eng. J. 168, 1279-1288 (2011).

[51] Langmuir, I.: The adsorption of gases on plane surfaces of glass, mica and platinum. J. Am. Chem. Soc. 40, 1361-140 (1918).

[52] Weber, T.W., Chakravorti, R.K.: Pore and solid diffusion models for fixed-bed adsorbers. AIChE J. 20, :228-238 (1974).

[53] Freundlich, H.: Uber die adsorption in lunsungen. J. Phys. Chem. 57, 385-470 (1907).

Table Headings

Table 1. Preparation of AC from PET by physical and chemical activation methods. Process yield and sample notations.

Table 2. Textural characterization of AC by the N_2 adsorption at -196ºC. Surface area and pore volumes.

Table 3. Textural characterization of AC by mercury porosimetry and density measurements. Pore volumes and mercury densities.

Table 4. pH_{pzc} values for the AC samples.

Table 5. Fitting of the experimental kinetic data to the pseudo-first and pseudo-second order kinetic models.

Table 6. Fitting of the experimental equilibrium data to the Freundlich and Langmuir models.

Captions to figures

Figure 1. pH_{pzc} measurement.

Figure 2. Adsorption isotherms for N_2 at -196 °C.

Figure 3. Curves of mercury intrusion.

Figure 4. FT-IR spectra for selected AC samples.

Figure 5. Adsorption kinetic of BPA for selected AC samples.

Figure 6. Adsorption isotherms of BPA for selected AC samples.

Table 1. Preparation of AC from PET by physical and chemical activation methods. Process yield and sample notations.

Aa	I_p	I_T/ºC	I_t/h	T/ºC	S_t/h	I_Y/%	A_Y/%	Notation
Steam	-	-	-	900	1	-	5.9	VA
KOH	1:1	85	2	850	2	96.0	58.4	KL1:1
KOH	1:3	85	2	850	2	93.1	48.3	KL1:3
KOH	1:5	85	2	850	2	75.8	49.4	KL1:5
KOH	1:1	-	-	850	2	-	75.8	KS1:1
KOH	1:3	-	-	850	2	-	38.1	KS1:3
KOH	1:5	-	-	850	2	-	23.9	KS1:5

Abbreviations: Aa, activating agent; I_p, impregnation ratio (PET:KOH); I_T, impregnation treatment temperature; I_t, impregnation treatment time; T, maximum heat treatment temperature (MHTT); S_t, soaking time at MHTT; I_Y, impregnation process yield; A_Y, activation process yield.

Table 2. Textural characterization of AC by the N_2 adsorption at -196ºC. Surface area and pore volumes.

Sample	$S_{BET}/m^2\,g^{-1}$	$W_0/cm^3\,g^{-1}$	$V_{mi}/cm^3\,g^{-1}$	$V_{me}/cm^3\,g^{-1}$
VA	1061	0.47	0.49	0.34
KL1:1	125	0.06	0.05	0.07
KL1:3	27	0.01	0.01	0.04
KL1:5	12	0.00	0.00	0.03
KS1:1	1060	0.41	0.42	0.19
KS1:3	1564	0.58	0.60	0.27
KS1:5	1990	0.71	0.55	0.73

Abbreviations: S_{BET}, BET surface area; W_0, micropore volume (Dubinin-Radushkevich); V_{mi}, micropore volume; V_{me}, mesopore volume.

Table 3. Textural characterization of AC by mercury porosimetry and density measurements. Pore volumes and mercury densities.

Sample	$V_{me\text{-}p}/cm^3\,g^{-1}$	$V_{ma\text{-}p}/cm^3\,g^{-1}$	$\rho_{Hg}/g\,cm^{-3}$	$\rho_{Hg}^{-1}/cm^3\,g^{-1}$	$V'_T/cm^3\,g^{-1}$
VA	0.36	0.08	1.24	0.81	0.91
KL1:1	0.13	0.38	0.87	1.15	0.57
KL1:3	0.10	0.35	0.99	1.01	0.46
KL1:5	0.08	0.35	0.95	1.05	0.43
KS1:1	0.31	1.49	0.40	2.50	2.21
KS1:3	0.56	2.11	0.31	3.23	3.25
KS1:5	0.81	1.77	0.35	2.86	3.29

Abbreviations: $V_{me\text{-}p}$, mesopore volume; $V_{ma\text{-}p}$, macropore volume; ρ_{Hg}, mercury density; $V'_T = W_0 + V_{me\text{-}p} + V_{ma\text{-}p}$, total pore volume. W_0, micropore volume (Dubinin-Radushkevich) from adsorption isotherms for N_2 at -196 ºC; $V_{me\text{-}p}$ and $V_{ma\text{-}p}$ from the curve of mercury intrusion.

Table 4. pH_{pzc} values for the AC samples.

Sample	pH_{pzc}
VA	7.20
KL1:1	6.35
KL1:3	6.37
KL1:5	6.25
KS1:1	5.60
KS1:3	5.35
KS1:5	5.70

Table 5. Fitting of the experimental kinetic data to the pseudo-first and pseudo-second order kinetic models.

		Pseudo-first order				Pseudo-second order		
Sample	t_e/h	$q_{e(theoretical)} \cdot 10^4$/ mol g^{-1}	$q_e \cdot 10^4$/ mol g^{-1}	k_1/ h^{-1}	R	$q_e \cdot 10^4$/ mol g^{-1}	k_2/ g mol^{-1} h^{-1}	R
VA	48	19.66	17.37	0.04	0.992	20.64	59	0.996
KS 1:1	96	12.31	6.40	0.02	0.921	12.31	319	0.999
KS 1:3	144	22.83	9.47	0.03	0.953	22.87	222	0.999
KS 1:5	144	21.99	5.48	0.02	0.848	22.08	526	1.000

Abbreviations: t_e, equilibrium time; q_e, amounts adsorbed at equilibrium; k_1, pseudo-first order rate constant; k_2, rate constant of pseudo-second order adsorption; R, fitting coefficient.

Table 6. Fitting of the experimental equilibrium data to the Freundlich and Langmuir models.

	Langmuir					Freundlich	
Sample	$Q_0 \cdot 10^3$/ mol g^{-1}	$b \cdot 10^{-3}$/ L mol^{-1}	R_L	R	1/n	$K_F \cdot 10^3$/ (mol g^{-1})/(mol L^{-1})$^{1/n}$	R
VA	2.62	15.60	0.060	0.999	0.50	118.88	0.784
KS1:1	1.11	8.50	0.105	0.668	2.37	-	0.811
KS1:3	2.15	84.71	0.012	0.999	0.10	4.39	0.973
KS1:5	4.25	10.84	0.084	1.000	0.26	25.51	0.983

Abbreviations: Q_0, maximum monolayer coverage capacity; b, Langmuir isotherm constant; n, adsorption intensity; K_F, Freundlich isotherm constant; R, fitting coefficient.

Figure 1. pH_{pzc} measurement.

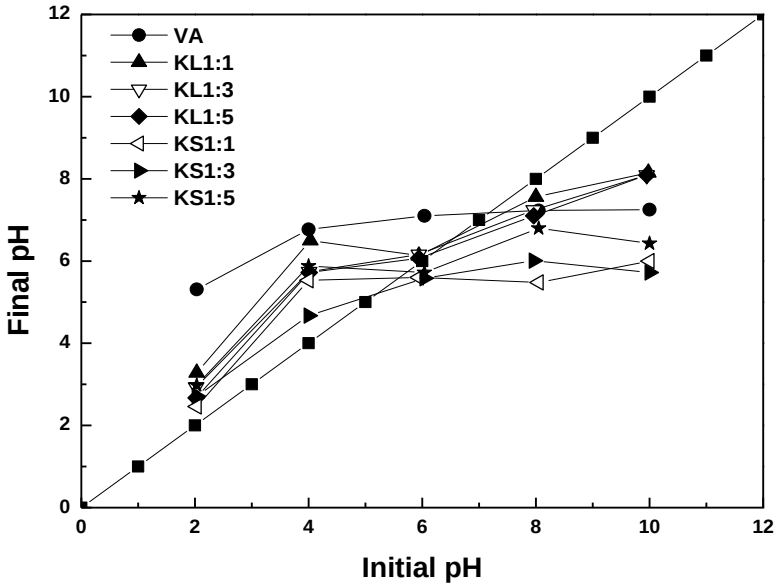

Figure 2. Adsorption isotherms for N_2 at -196 °C.

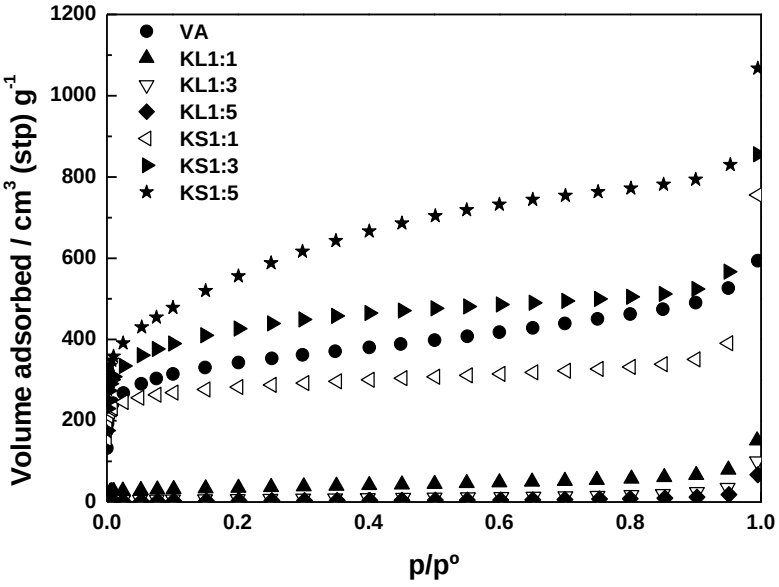

Figure 3. Curves of mercury intrusion.

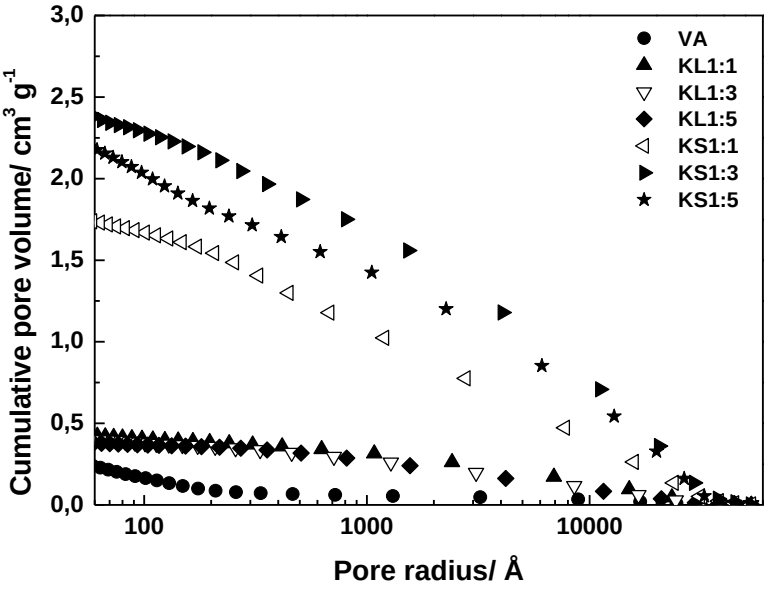

Figure 4. FT-IR spectra for selected AC samples.

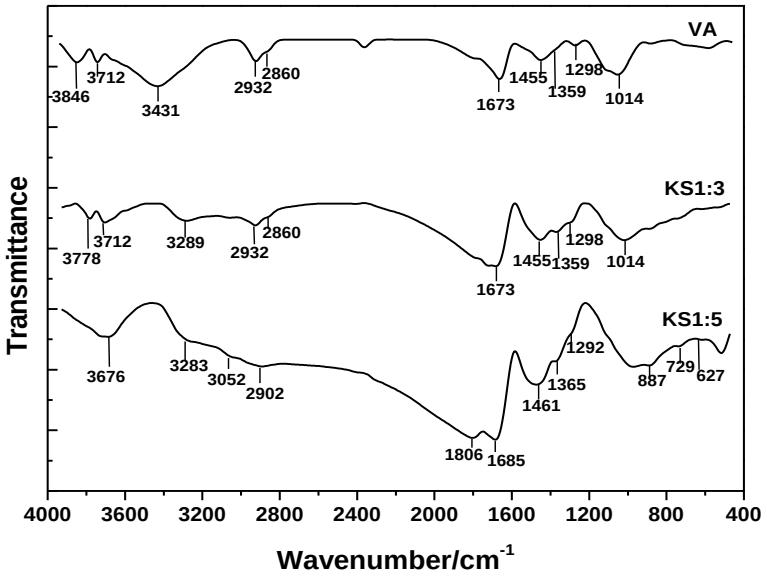

Figure 5. Adsorption kinetic of BPA for selected AC samples.

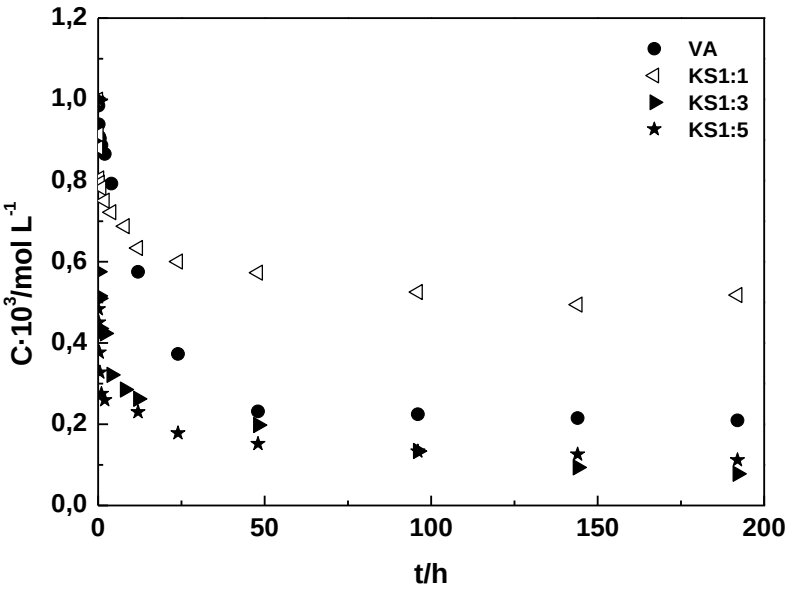

Figure 6. Adsorption isotherms of BPA for selected AC samples.